Predicting soil organic matter stability in agricultural fields through carbon and nitrogen stable isotopes

De Clercq, Tim[a]; Heiling, Maria[b]; Dercon, Gerd[b]; Resch, Christian[b]; Aigner, Martina[b]; Mayer, Leo[b]; Mao, Yanling[c]; Elsen, Annemie[d]; Steier, Peter[e], Leifeld, Jens[f]; Merckx, Roel[a]

[a] Division of Soil and Water Management, Department of Earth and Environmental Sciences, KU Leuven, Kasteelpark Arenberg 20, 3001 Heverlee, Belgium

[b] Soil and Water Management & Crop Nutrition Laboratory, Joint FAO/IAEA Division of Nuclear Techniques in Food and Agriculture, Department of Nuclear Sciences and Applications, International Atomic Energy Agency, Vienna, Austria

[c] Department of Resources and Environmental Sciences, Fujian Agriculture and Forestry University, Fujian, China

[d] Soil Service of Belgium, Willem de Croylaan 48, BE-3001 Leuven, Belgium

[e] Isotope Research and Nuclear Physics, VERA Laboratory, University of Vienna, Vienna, Austria

[f] Climate / Air Pollution Group, Agroscope, Institute for Sustainability Sciences ISS, Zürich, Switzerland

Corresponding author:

Tim De Clercq

Division of Soil and Water Management
Department of Earth and Environmental Sciences
KU Leuven
Kasteelpark Arenberg 20
3001 Heverlee, Belgium

Tel. +32 16 37 66 22

Tim.declercq@ees.kuleuven.be

Abstract

In order to evaluate the sustainability and efficiency of soil carbon sequestration measures and the impact of different management and environmental factors, information on soil organic matter (SOM) stability and mean residence time (MRT) is required. However, this information on SOM stability and MRT is expensive to determine via radiocarbon dating, precluding a wide spread use of stability measurements in soil science. In this paper, we test an alternative method, first developed by Conen et al. (2008) for undisturbed Alpine grassland systems, using C and N stable isotope ratios in more frequently disturbed agricultural soils. Since only information on carbon and nitrogen concentrations and their stable isotope ratios is required, it is possible to estimate the SOM stability at greatly reduced costs compared to radiocarbon dating. Using four different experimental sites located in various climates and soil types, this research proved the effectiveness of using the C/N ratio and $\delta^{15}N$ signature to determine the stability of mOM (mineral associated organic matter) relative to POM (particulate organic matter) in an intensively managed agro-ecological setting. Combining this approach with $\delta^{13}C$ measurements allowed discriminating between different management (grassland vs cropland) and land use (till vs no till) systems. With increasing depth the stability of mOM relative to POM increases, but less so under tillage compared to no-till practises. Applying this approach to investigate SOM stability in different soil aggregate fractions, it corroborates the aggregate hierarchy theory as proposed by Six et al. (2004) and Segoli et al. (2013). The organic matter in the occluded micro-aggregate and silt & clay fractions is less degraded than the SOM in the free micro-aggregate and silt & clay fractions. The stable isotope approach can be particularly useful for soils with a history of burning and thus containing old charcoal particles, preventing the use of ^{14}C to determine the SOM stability.

1. Introduction

Soils play a major role in the global carbon (C) cycle. The terrestrial soil organic carbon (SOC) pool contains about two and a half times more organic C than the vegetation and about twice as much C as is present in the atmosphere (Batjes, 1998). Down to a depth of 1 m the soil is estimated to contain 1500 Pg C (Batjes, 1996). Despite their low C concentrations, subsoil horizons are estimated to contain half of this C pool (Schmidt et al., 2011). Over the last 150 years cultivation and disturbance of agricultural soils have caused a net loss of between 40 and 90 Pg C globally (Lal and Bruce, 1999; Lal, 2004). These losses can be replenished by restoring degraded soils, converting marginal agricultural soils to restorative land use and adopting recommended management practices (Lal, 2004). Replenishing these C stocks has multiple benefits, for example increasing soil health and sequestering atmospheric CO_2. Considering agricultural land alone, approximately 5.5-6.0 Gt CO_2 eq. could potentially be stored each year, which amounts to approximately one sixth of global annual CO_2 emissions. (Olivier et al., 2012; Smith et al., 2008).

However, in order to evaluate the sustainability and efficiency of soil carbon sequestration measures and the impact of different management and environmental factors, information on soil organic matter (SOM) stability and mean residence time (MRT) is required. Since SOM stabilization is a combination of short- and long-term processes, any disturbance of these processes may result in the decomposition of young and old SOM alike (Lal et al., 2012; Schmidt et al., 2011). Agricultural soils can thus turn from a carbon sink into a carbon source very rapidly. A clear example is the conversion of tropical peat soils into agricultural land causing a massive CO_2 release due to profile drainage and subsequent oxidation of the stabilized SOM (Hooijer et al., 2010). In various parts of Western Europe knowledge of SOM stability is also needed for a different reason. SOM decomposition entails a release of mineral nitrogen and excess nitrogen can leach to surface- and groundwater causing eutrophication.

While historically, nitrogen release from SOM has been mastered adequately by empirical models, the more recent trends in (i) higher amendments of organic sources of nutrients like composts and (ii) changes in soil tillage techniques seem to have changed the distribution of SOM among fractions of different stability, possibly leading to a changed nitrogen release.

Radiocarbon dating is one of the only tools useable to study SOM dynamics on decadal to millennial timescales. The SOM ^{14}C content provides information on the time since C was fixed from the atmosphere and as such on SOM stability and MRT (Trumbore, 2009). However, this method is expensive, precluding a wide spread use of stability measurements in soil science. Conen et al. (2008) developed an alternative model to estimate the SOM stability of an Alpine, permanent grassland at steady state conditions. This model is based on the isotopic fractionation of the heavy stable isotope of nitrogen (^{15}N) during decomposition, which goes hand in hand with a decreasing C:N ratio during organic matter degradation. Due to the decreasing C:N ratio during litter decomposition and SOM formation as described in Figure 1, excess mineral N is released by soil micro-organisms. Isotopic fractionation during this nitrogen dissimilation and export process results in the preferential loss of the lighter ^{14}N from the SOM, leading to a highly ^{15}N enriched and stable SOM fraction (Coyle et al., 2009; Dijkstra et al., 2008). Since only information on carbon and nitrogen concentrations and their stable isotope ratios is required, it is possible to estimate the SOM stability at greatly reduced costs compared to radiocarbon dating. To date this model has only been tested under non-agricultural, undisturbed conditions. In this paper the validity of the above concepts will be tested in more frequently disturbed agricultural soils.

Insert Figure 1

Alternatively – in specific cases like C_3/C_4 vegetation changes - the ^{13}C content of SOM can be used to gain information on stability and MRT. A shift in cover crops from C_3 to C_4 plants changes the $\delta^{13}C$ signal of the inputs, which can then be traced in the SOM to calculate the MRT (Balesdent and Balabane, 1992; Balesdent and Mariotti, 1987; Collins et al., 1999). Unfortunately this C_3-C_4 shift is not always present at the site of interest. However, the ^{13}C content of organic matter also increases upon microbial degradation, without cropping changes and is most visible with increasing depth (Rumpel and Kögel-Knabner, 2011). As both C and N isotope ratios are influenced by microbial degradation, integrating the $\delta^{13}C$ signature into the model could increase the accuracy of the SOC stability estimation. To our knowledge no attempt has been made yet to combine carbon and nitrogen stable isotope ratios as a proxy for SOM stability.

Moreover the simple two pool model used by Conen et al. (2008) only yields limited information on the nature of the stabilization mechanisms involved. While SOM stability and protection are governed by the interaction of biochemical recalcitrance, adhesion to soil mineral particles and physical protection from degradation through particle aggregation, no general consensus exists on fractionation methods for estimating SOM stability (Jandl et al., 2013; Six et al., 2002b). Thus, in order to obtain a more detailed picture of the protection mechanisms involved in SOM stabilization five SOM pools with varying degrees of physical and (bio)chemical protection were isolated based on the fractionation scheme developed by Six et al. (2002a). The principles for determining SOM stability outlined above were applied to these fractions to gain better understanding of SOM stability and its link with aggregate formation.

To summarize, this study has three main goals. We will test the hypothesis that the C:N ratio and $\delta^{15}N$ signature can be used as a proxy for SOM stability in a disturbed agricultural setting. To achieve this the procedure and model described by Conen et al. (2008) will be followed. Secondly, it is tested if the $\delta^{13}C$ depth profile of the study sites can enhance the performance of the model and provide additional information on the degree of SOM stabilization. Thirdly, the application of the C:N ratio and ^{15}N isotope model is linked to a more elaborate soil fractionation scheme based on Six et al. (2002). This will yield a better understanding of SOM dynamics and soil aggregate formation under different management practices. These hypotheses were tested on four long-term field experiments, established on soils poor and rich in soil organic matter in Austria and Belgium.

2. Materials and Methods

2.1. Site description

Soil samples were taken from four long term agricultural fields on two locations in Austria and two in Belgium. The sites were selected for their diverse management, climatic and soil characteristics and because a detailed cultivation history was available. The climatic and soil characteristics of these four experimental sites can be found in Table 1.

Insert Table 1

In Austria we selected a site in Gross-Enzersdorf and one in Grabenegg, both in the region of Lower Austria. On the former site a tillage experiment with crop rotation including winter wheat, sugar beet and corn started in 1997. This experiment includes five treatments: a conservation tillage, two conventional tillage and two mulching treatments. The plots measure 40m by 24m. Strips of permanent grassland were established in between these treatments as a buffer. For this study, samples were taken from the conservation tillage treatment (strictly no-till) and conventional tillage treatment (plough depth of 25 to 30cm) and samples from the permanent grass alleys served as a baseline control.

The Grabenegg site has been continuously used for crop production until permanent grassland was established in 1997. After 15 years, in 2012, the grassland was tilled and reconverted to cropland. Immediately after tilling samples were taken on nine contours along the slope of the field to a depth of 1m.

In Belgium two sites were selected, in Boutersem and in Gembloux, both in the Belgian loam belt. On the former site a long term vegetable, fruit and garden (VFG) compost application trial was set up in 1997 with a five year crop rotation cycle, including potatoes, sugar beet, winter wheat and carrots. The five treatments sampled for this experiment are: an unfertilized control, a mineral fertilized control, a three-yearly application of VFG-compost comprising of 45 tons per hectare and two yearly applications of VFG compost comprising of 15 and 45 tons per hectare. The experiment was laid out in a randomized block design in 4 replicates and with plots of 10 by 10.5m (Tits et al., 2012). The compost contained 14.4 ± 3.8 % carbon and 1.4 ± 0.3 % nitrogen. The average $\delta^{13}C$ value was -28.7 and the $\delta^{15}N$ value 8.1.

Since 1959 the Centre de Recherche Agronomique de Gembloux conducts a long term agricultural trial on the evolution of SOC stocks on a site in Gembloux. This site has a rotation consisting of sugar beet followed by two or three years of cereals. The plots measure 10 by 24m and are laid out in a randomized block design (Van Wesemael et al., 2004). Samples were taken in four replicates on a mineral fertilized control (crop residues exported), a treatment with application of stable manure every four years (crop residues exported) and two treatments were crop residues were incorporated in the soil, one with and without green manure.

2.2. Sampling procedure

Both Belgian trials were sampled in February 2012. In each of four replicates of all sampled treatments eight soil cores were taken 2m apart, from 0-30cm depth and mixed to form a composite sample. The samples were dried at 45°C, crushed and sieved to < 2mm or < 8 mm, depending on the subsequent fractionation scheme. In November 2011 samples were taken in

Gross-Enzersdorf and in March 2012 in Grabenegg. In each of three replicates of all sampled treatments 12 soil cores were taken up to 1m depth, spaced over the plots. A composite sample was formed for each of the three replicates for eight depth layers: 0-5, 5-10, 10-15, 15-20, 20-40, 40-60, 60-80 and 80-100 cm. All samples were dried at 40°C, crushed and sieved to < 2 mm.

2.3. SOC fractionation

A particulate organic matter fraction (POM) larger than 63µm (Austrian samples) and 53µm (Belgian samples) and lighter than 1.8 g cm^{-3} was obtained by a combination of ultrasonic dispersion with an energy of 22 J cm^{-3}, wet sieving and density separation according to the procedure described by Zimmermann et al. (2007) and Conen et al. (2008). This was done for three depths, 0-5cm, 10-15cm and 40-60cm for the Austrian soils and on the 0-30cm soil layer for the Belgian soils. The mOM fraction was calculated as the difference between the bulk soil weight and the POM. This procedure leads to the inclusion of the labile dissolved organic carbon (DOC) in the calculated mOM fraction. But based on drying-rewetting experiments conducted by Merckx et al. (2001) it was calculated that this DOC only constitutes 0.1% of the mOM fraction carbon and as such has no significant influence on the results.

An alternative fractionation scheme, based on Six et al. (2002a), was also used on the Belgian soils. It distinguishes five SOM pools with varying degrees of physical and (bio)chemical protection as illustrated in Figure 2. Subsequently, 8 mm sieved soil is passed over a 250µm and 53µm sieve, yielding a macro-aggregate fraction (M) larger than 250µm, a free micro-aggregate fraction (m) between 250 and 53µm and a free silt & clay faction (s+c) smaller than 53µm. Afterwards the M fraction is passed through the micro-aggregate isolator, a devise that breaks the macro-aggregates using small glass beads. The occluded silt & clay faction (s+c M) and occluded micro-aggregate fraction (mM) are washed through a 250 µm mesh by a constant water stream, the POM (larger than 250µm) fraction is left on top. The mM and s+c

M fractions are subsequently separated by a 53µm sieve. The procedure is described in detail by Six et al. (2002a).

Insert Figure 2

2.4. Isotopic analysis

Carbon and nitrogen content and their respective stable isotope ratios were analyzed for the POM fraction and bulk soil with an elemental analyzer (Flash 2000, Thermo Scientific, Massachusetts, USA) coupled with a mass spectrometer (Isoprime GV Instruments, Manchester, UK). The samples from the Gross-Enzersdorf soil were fumigated to remove carbonates, all other soils were free of carbonates. For the protected mineral associated organic matter fraction (mOM), carbon and nitrogen content were calculated as the difference between the bulk soil and the POM. The samples of the fractionation scheme based on Six et al. (2002a) (m, mM, s+c, s+cM, POM and bulk soil) were also analyzed with an elemental analyzer (Flash 2000, Thermo Scientific, Massachusetts, USA) coupled with a mass spectrometer (Isoprime GV Instruments, Manchester, UK).

2.5. Data analysis and calculations

To calculate the relative stability of the SOC, the following three equations (1, 2 and 3) developed by Conen et al. (2008) were used. In these equations δ_m and δ_p are the $\delta^{15}N$ value for the mOM and POM respectively, ε [‰] is the enrichment factor, r_m and r_p are the C:N ratio's and C_m and C_p the carbon masses for the mOM and POM fraction respectively. f_N and f_C are the fractions of nitrogen and carbon lost during degradation. And η is the relative SOM stability.

$$f_N = 1 - e^{\left(\frac{\delta_m - \delta_p}{\varepsilon}\right)} \quad (1)$$

$$f_C = f_N + (1 - f_N) \cdot \left(1 - \left(\frac{r_m}{r_p}\right)\right) \quad (2)$$

$$\eta = \frac{c_m}{c_p \cdot (1 - f_C)} \quad (3)$$

The statistical package R 3.0.1 (R core team, 2013) was used for all data analysis. To determine significant effects and interactions, ANOVA was applied. Duncan's new multiple range test was used to test equality of treatment averages. Averages followed by the same letter do not significantly differ from each other with a certainty of more than 95%.

The multivariate analysis was done in JMP Pro 11.0.0, SAS Institute Inc., Cary, NC. Principle components analysis was used to calculate principal components and score coefficients.

3. Results

3.1. C:N ratio and $\delta^{15}N$ in POM and mOM

In the following Figure 3 the C:N ratio and $\delta^{15}N$ signature of the isolated SOC fractions are displayed for all four research sites. For all four sites our first hypothesis is confirmed, the pattern of the C:N ratio and $\delta^{15}N$ signature closely resembles the predicted theoretical pattern from Figure 1.

In Figure 3a the average results for all nine sampled contours, at three depths, of the site in Grabenegg can be seen. At all three depths the POM has a higher C:N ratio and a lower $\delta^{15}N$ signature compared to the mOM fraction. The POM isolated from the soil layer between 40 and 60 cm deep has the highest C:N ratio of all the fractions, the POM from the two top soil layers does not have a significantly different signature. The variation of both parameters is also by far the highest in the deep soil POM.

Insert Figure 3

In Gross-Enzersdorf (Figure 3b) the same pattern for the POM and mOM fraction can be observed as in Grabenegg. The POM in both top soil layers has a lower C:N ratio compared to the deep soil layer. The $\delta^{15}N$ signature of the POM shows a significant interaction between treatment and depth. For the conventional tillage treatment it decreases with depth, for both other treatments it increases. The largest variations for both parameters can be found in the grass alley treatment, for all depths. Overall the POM from deep soil layer displays the highest variability and the C:N ratio is considerably higher compared to the two top soil layers.

Figures 3c and 3d display the results for both Belgian soils. The same pattern of the fractions as seen in both Austrian soils emerges. For the site in Boutersem (Figure 3c) a significantly higher $\delta^{15}N$ signature and a lower C:N ratio is observed in both fractions from the compost application treatments as compared to the control. The mulch and control treatment of the site in Gembloux (Figure 3d) show no significant difference in $\delta^{15}N$ signature or C:N ratio.

In Table 2 the carbon concentration (in mg/g dry soil) of both isolated fractions, POM and mOM is summarized for all four experimental sites. In both Austrian sites the C concentration declines significantly with depth, the lowest concentrations are found in the 40-60 cm layers. For all sites and treatments, except for 45 tons compost $ha^{-1}y^{-1}$ in Boutersem, most of the carbon can be found in the mOM fractions. In Gross-Enzersdorf only the top layer POM reveals significant treatment effects, the carbon concentration is the highest in the alley treatment, followed by the conservation tillage and conventional tillage treatments. The same significant pattern can be seen in the mOM fractions for all depths. For the Boutersem site the only significant treatment effect can be found in the POM fraction, whereas in Gembloux only the carbon concentration in the mOM fraction shows an influence of the treatment.

Insert Table 2

3.2. SOM Relative stability

Using the data shown in Figure 3 and Table 2, the relative stability of the SOC was calculated according to equations 1, 2 and 3, based on Conen et al. (2008). For the enrichment factor ε the value of −2.0‰ was used, derived from literature (Conen et al., 2008; Robinson, 2001). The results are shown in Table 3. For the treatment factor no significant effect could be found in any of the sites, but some trends can be seen and are discussed in the next section. In the case of the Gross-Enzersdorf and Grabenegg sites, there is a significant depth effect, the relative SOM stability always increases deeper into the profile.

Insert Table 3

3.3. Relative stability and $\delta^{13}C$

To obtain additional information about the stability of the SOC a $\delta^{13}C$ depth profile was constructed for Grabenegg (data not show) and Gross-Enzersdorf (Figure 4). The $\delta^{13}C$ signature becomes more positive with increasing depth in all treatments, but the values and overall slopes differ significantly (p=0.0009 and slope is 0.0103 for conventional tillage, 0.0028 for conservation tillage and 0.0147 for grass alley). In both arable treatments the $\delta^{13}C$ signature only increases below the 20cm layer, whereas in the alley treatment it starts increasing immediately. Below 20cm the $\delta^{13}C$ signature under conventional tillage (slope 0.0148) increases significantly (p=0.0034) faster compared to both other treatments (slope alley 0.00944 and conservation 0.00614) .

Insert figure 4

To investigate the correlation of $\delta^{13}C$ with the other parameters and the SOM stability, a principal component (PC) analysis was performed on the data of both Austrian soils. A total of 16 parameters and 4 ratios were considered in the analysis. As a result, three independent and uncorrelated components, defined as linear combinations of the initial variables, were calculated. Table 4 shows the loadings matrix of the final three selected components. The higher the loading value the more variation of the variable is explained by the PC. The PC 1 is composed of depth, POM [N], POM [C], bulk soil [C], bulk soil [N], mOM [N], mOM [C], POM C:N ratio, η and the mOM/POM C:N ratio. PC 2 is composed of POM $\delta^{13}C$, bulk soil $\delta^{13}C$, mOM $\delta^{13}C$ and $\delta^{15}N$, mOM/POM $\delta^{13}C$, mOM C:N ratio and bulk C:N ratio. PC 3 is composed of all $\delta^{15}N$ variables. The three components together explain almost 80% of total variance.

Insert table 4

3.4. Relative stability and aggregate formation

The soil samples from both Belgian sites were further analyzed following the fractionation scheme in Figure 2. For three Boutersem treatments i.e. the unfertilized control, mineral fertilized control and 45t $ha^{-1}y^{-1}$ compost application and for three Gembloux treatments, control and mulch with and without green manure, the C/N ratio and $\delta^{15}N$ signature for five SOC fractions are displayed in Figure 5.

Insert Figure 5

In Figure 5a, the POM fraction of the compost application treatment has a lower C/N ratio and higher $\delta^{15}N$ signature compared to the control. This is also the case for the $\delta^{15}N$ signature of the two micro-aggregate and silt & clay fractions. The occluded fractions of both treatments have a lower $\delta^{15}N$ signature compared to the free fractions. The silt & clay fractions also always have a higher $\delta^{15}N$ signature compared to the associated micro-aggregate fractions.

In Figure 5b the pattern is slightly different. Here the POM fractions do not have the lowest $\delta^{15}N$ signature. The other fractions follow the same pattern as in Figure 5a.

4. Discussion

4.1. SOM relative stability

On all four research sites our primary hypothesis could be confirmed. Figure 3 shows that the C:N ratio and $\delta^{15}N$ signature can be used as a proxy for SOM degradation and stabilization in much more disturbed agricultural systems compared to the Alpine grasslands as researched by Conen et al. (2008). The sites described in this study are all long term agricultural sites with different management, tillage and fertilization practices.

Secondly it is observed that the ^{15}N signal of mineral fertilizer has no influence on this model, as no significant difference could be found in $\delta^{15}N$ signature of any fraction between the unfertilized control and the mineral fertilized treatment even though the applied calcium ammonium nitrate had a $\delta^{15}N$ signal of -0.40 (Boutersem, Figure 5a). This indicates it is possible to use the model developed by Conen et al. (2008) even in situations where mineral fertilizer is used.

Three main effects on SOM relative stability can be distinguished in this study: the influence of biomass input, tillage and depth. Looking at the relative stability no significant management effect could be found, but some clear trends can be seen. With increasing organic matter addition the stability of mOM relative to POM tends to decrease, as seen on the sites of Boutersem and Gembloux, although on the Boutersem site this effect can be partially due to the higher $\delta^{15}N$ value of the added compost (attributed to microbial degradation during the composting process). (Table 3).

In the case of the Gross-Enzersdorf experiment, the results are slightly more complex. The grass alley treatment, where biomass returns can be thought larger compared to both agricultural treatments (Vleeshouwers and Verhagen, 2002), has a slightly lower relative stability in the upper soil layer and an intermediate relative stability in the deeper layers, compared to both arable treatments (till and no till). For the alley and no-till treatments a clear and significant η increase is observed with increasing depth, whereas for the tillage treatment no clear increase is observed between 5 and 15 cm layers and a smaller increase is observed in the deepest soil layer. This difference can be attributed to the mixing of both top soil layers in the latter through ploughing.

Overall a significant increase in relative stability is observed from the top to deeper soil layers, also on the Grabenegg site. In the deeper soil layers, there is much less SOC (POM as well as mOM) as seen in Table 2 and it exhibits a larger variation in C:N ratio and $\delta^{15}N$ signature compared to the top soil, especially for the POM fraction. This is probably due to a more unequal horizontal distribution of the OM in the deep soil caused by preferential flow paths, plant routing behavior and bioturbation, as indicated by Rumpel and Kögel-Knabner (2011). The ratio of POM over mOM carbon is also much lower and this lack of fresh OM in the subsoil leads to nutrient and energy limitations and combined with suboptimal environmental conditions inhibits further microbial degradation, leading to a higher relative stability of the OM (Fontaine et al., 2007; Rumpel and Kögel-Knabner, 2011; Schmidt et al., 2011).

4.2. $\delta^{13}C$ as additional indicator of stability

As can be seen in Figure 4, the $\delta^{13}C$ signature under conventional tillage increases significantly faster below the 20cm zone, compared to both other treatments. This might be due to a hard plough pan situated at a depth of around 30cm which inhibits the supply of fresh OM (mainly root material) to the deeper soil layers. This is consistent with the observed lower carbon concentration in the 40-60cm layer in Table 2.

For both Austrian sites the bulk $\delta^{13}C$ signature is correlated with the relative stability η displayed in Figure 6. The correlation is best for the Gross-Enzersdorf grass alley treatment (R^2=0.70) and the Grabenegg site (R^2=0.74). Except for the conservation tillage treatment, $\delta^{13}C$ signature is always positively correlated with SOM relative stability. To further investigate the correlation of $\delta^{13}C$ with the other measured parameters and the SOM stability, a principal component analysis was performed on the data of both Austrian soils. The results can be seen in Table 4. Figure 7 shows the scores of the Austrian samples for the first two principal components, defined as a depth parameter and a land use parameter. Multiple clusters can be seen. The first cluster (I) contains all samples from the deepest soil layer (40-60cm). The other two clusters group the samples from the top soil layers. Cluster II contains the 10-15cm and the tilled 0-5cm samples. Cluster III contains the untilled 0-5 cm soil layer samples (Gross Enzersdorf no till and grass alley). On top of this we find a separation between the long term agricultural plots (top half) and those from the long term grassland plots (bottom half).

Insert Figure 6 and Figure 7

Combining the carbon and nitrogen concentrations and respective stable isotope ratios of the soil POM and mOM fractions offers an opportunity to distinguish SOM of different depths, management systems and land use systems, all of which have an impact on SOM stability. In Figure 7 the relative SOM stability increases from the bottom right to the top left as suggested by rotated factor pattern (Table 4) and confirmed by Figure 8. In this biplot the loadings of the factors used in the principle components analysis are displayed on top of the scores of the first two principle components. The arrow for η indicates it increases from the bottom right to the top left. This was not possible on the basis of the model by Conen *et al.* (2008) since they did not use $\delta^{13}C$ signature changes. This emphasizes the value of also using the $\delta^{13}C$ signature changes in a new mechanistic model based on that of Conen *et al.* (2008).

Insert Figure 8

4.3. Relative stability and Aggregate formation

Since it is known that SOM stability and protection are governed by the interaction of biochemical recalcitrance, adhesion to soil mineral particles and physical protection through particle aggregation, an alternative and more detailed fractionation scheme (Figure 2) was applied on both Belgian soils (Six et al., 2004, 2002b). The model developed by Conen et al. (2008) could not be applied on these fractions but the C:N ratio and $\delta^{15}N$ signature alone also supplied information on stability. Figure 5 demonstrated that the degree of microbial degradation increases in the following order: POM < occluded micro-aggregates < occluded silt & clay < free micro-aggregates < free silt & clay. This corroborates the aggregate formation theory as described by Six et al. (2004) and Segoli et al. (2013) where the fresh residue is converted to POM and serves as the core of newly formed macro-aggregates. Inside of these macro-aggregates the POM is further degraded and occluded micro-aggregates are formed. Part of the organic matter is bound to the mineral soil particles (silt & clay fraction) and part is incorporated in the newly formed micro-aggregates. After a while the macro-aggregates can disintegrate and the micro-aggregates and silt & clay particles are freed. This implies that the younger and intermediate SOM will be located in the POM and occluded fractions and the older in the free fractions, exactly as is determined using the C:N ratio and $\delta^{15}N$ signature.

Furthermore a clear influence of the different treatments on the C:N ratio and $\delta^{15}N$ signature can be seen on both sites. The long term application of compost, already partially degraded with an average C:N ratio of 8.5 and $\delta^{15}N$ of 8.1, pushes the signal of all isolated fractions to the bottom right of the graph. This indicates that the compost residue has been incorporated in all isolated fractions, over the course of 15 years.

4.4. Conclusions

Using four different experimental sites located in various climates and soil types, this research proved the effectiveness of using the C/N ratio and $\delta^{15}N$ signature to determine the stability of mOM relative to POM in an intensively managed agro-ecological setting. Combining this approach with $\delta^{13}C$ measurements allowed discriminating between different management (grassland vs cropland) and land use (till vs no till) systems. With increasing depth the stability of mOM relative to POM increases, but less so under tillage compared to no-till practices. Compost addition has a negative effect on the relative stability, probably because the compost added is already partially degraded during the composting process and mainly ends up in the POM fraction. Thus the difference with the mOM is smaller. Applying this approach to investigate SOM stability in different soil aggregate fractions, it corroborates the aggregate hierarchy theory as proposed by Six et al. (2004) and Segoli et al. (2013). The organic matter in the occluded micro-aggregate and silt & clay fractions is less stable than the SOM in the free micro-aggregate and silt & clay fractions. Hence, the model developed by Conen et al. (2008) has been proven valid for use in more intensively managed agricultural systems and could in the future be supplemented with a $\delta^{13}C$ component. It can be particularly useful for soils with a history of burning and thus containing old charcoal particles, preventing the use of ^{14}C to determine the SOM stability. Although further validation with radiocarbon dating on other soils and management systems and under different climates is needed, this stable isotope based approach can become a useful tool in future SOM stability research.

5. Acknowledgements

This research was initiated within the framework of the IAEA funded Coordinated Research Project (CRP) on *Soil Quality and Nutrient Management for Sustainable Food Production in Mulch-based Cropping Systems in Sub- Saharan Africa (CRP D1.50.12)*. Further research funding was obtained through a Ph.D. grant of the Flemish Agency for Innovation by Science and Technology (IWT). We also would like to thank our Austrian, Belgian and Swiss partners who provided access to the study sites and analytical support: the Austrian Agency for Health and Food Safety (AGES), the University of Natural Resources and Life Sciences Vienna (BOKU), the Climate and Air Pollution Group (Agroscope) of the Institute for Sustainability Sciences in Zürich, the VERA Laboratory of the University of Vienna, the Soil Service of Belgium (BDB) and the Centre Wallon de Recherches Agronomiques (CRA-W). The following members of the Soil and Water Management & Crop Nutrition Laboratory, Joint FAO/IAEA Division of Nuclear Techniques in Food and Agriculture were also instrumental in the success of this research: Jose Arrillaga, Arsenio Toloza, Norbert Jagoditsch, Franz Augustin.

6. References

Balesdent, J., Balabane, M., 1992. Maize root-derived soil organic carbon estimated by natural 13C abundance. Soil Biol. Biochem. 24, 97–101.

Balesdent, J., Mariotti, A., 1987. Natural 13C abundance as a tracer for studies of soil organic matter dynamics. Soil Biol. Biochem. 19, 25–30.

Batjes, N.H., 1996. Total carbon and nitrogen in the soils of the world. Eur. J. Soil Sci. 47, 151–163.

Batjes, N.H., 1998. Mitigation of atmospheric CO 2 concentrations by increased carbon sequestration in the soil. Biol. Fertil. Soils 27, 230–235.

Collins, H., Blevins, R., Bundy, L., Christenson, D., Dick, W., Huggins, D., Paul, E., 1999. Soil carbon dynamics in corn-based agroecosystems: Results from carbon-13 natural abundance. Soil Sci. Soc. Am. J. 63, 584–591.

Conen, F., Zimmermann, M., Leifeld, J., Seth, B., Alewell, C., 2008. Relative stability of soil carbon revealed by shifts in? 15 N and C: N ratio. Biogeosciences 5, 123–128.

Coyle, J.S., Dijkstra, P., Doucett, R.R., Schwartz, E., Hart, S.C., Hungate, B. a., 2009. Relationships between C and N availability, substrate age, and natural abundance 13C and 15N signatures of soil microbial biomass in a semiarid climate. Soil Biol. Biochem. 41, 1605–1611.

Dijkstra, P., LaViolette, C.M., Coyle, J.S., Doucett, R.R., Schwartz, E., Hart, S.C., Hungate, B. a, 2008. 15N enrichment as an integrator of the effects of C and N on microbial metabolism and ecosystem function. Ecol. Lett. 11, 389–97.

Fontaine, S., Barot, S., Barré, P., Bdioui, N., Mary, B., Rumpel, C., 2007. Stability of organic carbon in deep soil layers controlled by fresh carbon supply. Nature 450, 277–80.

Hooijer, a., Page, S., Canadell, J.G., Silvius, M., Kwadijk, J., Wösten, H., Jauhiainen, J., 2010. Current and future CO2 emissions from drained peatlands in Southeast Asia. Biogeosciences 7, 1505–1514.

Jandl, R., Rodeghiero, M., Martinez, C., Cotrufo, M.F., Bampa, F., van Wesemael, B., Harrison, R.B., Guerrini, I.A., Richter, D.D., Rustad, L., Lorenz, K., Chabbi, A., Miglietta, F., 2013. Current status, uncertainty and future needs in soil organic carbon monitoring. Sci. Total Environ. 468-469C, 376–383.

Lal, R., 2004. Soil carbon sequestration to mitigate climate change. Geoderma 123, 1–22.

Lal, R., Bruce, J.P., 1999. The potential of world cropland soils to sequester C and mitigate the greenhouse effect. Environ. Sci. Policy 2, 177–185.

Lal, R., Lorenz, K., Hüttl, R.F., Schneider, B.U., von Braun, J. (Eds.), 2012. Recarbonization of the Biosphere. Springer Netherlands, Dordrecht.

Merckx, R., Brans, K., Smolders, E., 2001. Decomposition of dissolved organic carbon after soil drying and rewetting as an indicator of metal toxicity in soils. Soil Biol. Biochem. 33, 235–240.

Olivier, J.G.J., Janssens-Maenhout, G., Peters, J.A.H.W., 2012. Trends in global CO2 emissions; 2012 Report. The Hague/Bilthoven.

Robinson, D., 2001. δ15N as an integrator of the nitrogen cycle. Trends Ecol. Evol. 16, 153–162.

Rumpel, C., Kögel-Knabner, I., 2011. Deep soil organic matter—a key but poorly understood component of terrestrial C cycle. Plant Soil 338, 143–158.

Schmidt, M.W.I., Torn, M.S., Abiven, S., Dittmar, T., Guggenberger, G., Janssens, I. a, Kleber, M., Kögel-Knabner, I., Lehmann, J., Manning, D. a C., Nannipieri, P., Rasse, D.P., Weiner, S., Trumbore, S.E., 2011. Persistence of soil organic matter as an ecosystem property. Nature 478, 49–56.

Segoli, M., De Gryze, S., Dou, F., Lee, J., Post, W.M., Denef, K., Six, J., 2013. AggModel: A soil organic matter model with measurable pools for use in incubation studies. Ecol. Modell. 263, 1–9.

Six, J., Bossuyt, H., Degryze, S., Denef, K., 2004. A history of research on the link between (micro)aggregates, soil biota, and soil organic matter dynamics. Soil Tillage Res. 79, 7–31.

Six, J., Callewaert, P., Lenders, S., De Gryze, S., Morris, S.J., Gregorich, E.G., Paul, E.A., Paustian, K., 2002a. Measuring and understanding carbon storage in afforested soils by physical fractionation. Soil Sci. Soc. Am. J. 66, 1981–1987.

Six, J., Conant, R., Paul, E., Paustian, K., 2002b. Stabilization mechanisms of soil organic matter: Implications for C-saturation of soils. Plant Soil 241, 155–176.

Smith, P., Martino, D., Cai, Z., Gwary, D., Janzen, H., Kumar, P., McCarl, B., Ogle, S., O'Mara, F., Rice, C., Scholes, B., Sirotenko, O., Howden, M., McAllister, T., Pan, G., Romanenkov, V., Schneider, U., Towprayoon, S., Wattenbach, M., Smith, J., 2008. Greenhouse gas mitigation in agriculture. Philos. Trans. R. Soc. Lond. B. Biol. Sci. 363, 789–813.

Tits, M., Elsen, a., Bries, J., Vandendriessche, H., 2012. Short-term and long-term effects of vegetable, fruit and garden waste compost applications in an arable crop rotation in Flanders. Plant Soil.

Trumbore, S., 2009. Radiocarbon and Soil Carbon Dynamics. Annu. Rev. Earth Planet. Sci. 37, 47–66.

Van Wesemael, B., Lettens, S., Roelandt, C., Van Orshoven, J., 2004. Changes in soil carbou stocks from 1960 to 2000 in the main Belgian cropland areas. Biotechnol. Agron. Société Environ. 8, 133–139.

Vleeshouwers, L.M., Verhagen, a., 2002. Carbon emission and sequestration by agricultural land use: a model study for Europe. Glob. Chang. Biol. 8, 519–530.

Zimmermann, M., Leifeld, J., Schmidt, M.W.I., Smith, P., Fuhrer, J., 2007. Measured soil organic matter fractions can be related to pools in the RothC model. Eur. J. Soil Sci. 58, 658–667.

Table 1

Table 1: Site characteristics for all four long term experimental fields used in this study.

Site	Austria		Belgium	
	Gross-Enzersdorf	Grabenegg	Boutersem	Gembloux
Annual rainfall	554 mm	686 mm	760 mm	828 mm
Average temp.	9.8°C	8.4°C	11°C	9.8°C
Min. monthly temp.	-2.9°C	-2.8°C	-1.5°C	-0.4°C
Max. monthly temp.	26.0°C	24.9°C	20.6 °C	22.1°C
Climate	humid continental (Dfb)		temperate oceanic (Cfb)	
Soil type	Chernozem	Luvisol	Cambisol	Luvisol
pH ($CaCl_2$)	7.5	6.7	6.4	6.2
Parent material	loess	loess	sandy-loam colluvium	loess

Table 2

Table 2: Carbon concentration (mg/g dry soil) for SOC fractions from the Grabenegg, Gross-Enzersdorf, Boutersem and Gembloux experimental sites. Treatment means ± standard deviations and F-test p-values are presented.

			[C] (mg/g dry soil)					
			POM			**mOM**		
			0-5 cm	**10-15 cm**	**40-60 cm**	**0-5 cm**	**10-15 cm**	**40-60 cm**
Gross-Enzersdorf	Till		0.87 ± 0.07	0.87 ± 0.19	0.08 ± 0.06	18.11± 2.25	17.59 ± 2.3	6.54 ± 4.2
	No till		2.46 ± 1.04	0.48 ± 0.1	0.11 ± 0.01	22.63± 1.0	19.62± 1.27	11.53 ± 0.87
	Alley		3.32 ± 0.17	0.75 ± 0.06	0.1 ± 0.05	24.6 ± 0.5	18.05± 1.3	10.23± 4.64
	F test	Treatment	*8.98e-10*			*1.03e-08*		
		Depth	*0.0009*			*0.0064*		
		Interaction	*<0.001*			*ns*		
Grabenegg	Average		0.92 ± 0.22	1.2 ± 0.17	0.09 ± 0.04	12.3 ± 1.28	13.38 ± 1.19	4.31 ± 0.87
	F test	Depth	*<0.001*			*<0.001*		
			0-30 cm			**0-30 cm**		
Gembloux	Control		0.54 ± 0.25			7.01 ± 0.21		
	Mulch		0.68 ± 0.2			7.54 ± 0.08		
	F test	Treatment	*ns*			*0.015*		
Boutersem	Control		1.08 ± 0.43			6.53 ± 0.7		
	15 tons compost $ha^{-1}y^{-1}$		2.49 ± 0.96			9.49 ± 0.6		
	45 tons compost $ha^{-1}y^{-1}$		10 ± 3.75			7 ± 4.14		
	F test	Treatment	*0.006*			*ns*		

Table 3

Table 3: The relative stability (η) of SOC from the Grabenegg, Gross-Enzersdorf, Boutersem and Gembloux experimental sites. Treatment means ± standard deviations are presented, values followed by different letters differ significantly from each other.

			η (relative SOM stability)		
			0-5 cm	**10-15 cm**	**40-60 cm**
Gross-Enzersdorf	Till		129 ± 4	170 ± 53	494 ± 146
	No till		106 ± 69	291 ± 100	1012 ± 473
	Alley		91 ± 23	230 ± 65	877 ± 397
	F test	Treatment	*ns*		
		Depth	*<0.001*		
		Interaction	*ns*		
Grabenegg	Average		71 ± 15	54 ± 17	358 ± 114
	F test	Depth	*<0.001*		
			0-30 cm		
Gembloux	Control		129 ± 101		
	Mulch		62 ± 36		
	F test	Treatment	*ns*		
Boutersem	Control		28 ± 23		
	15 tons compost $ha^{-1}y^{-1}$		12 ± 7		
	45 tons compost $ha^{-1}y^{-1}$		2 ± 1		
	F test	Treatment	*ns*		

Table 4

Table 4: Rotated PC pattern for SOC properties of experimental sites in Gross-Enzersdorf and Grabenegg (n=42).

Variable	**PC 1 (depth)**	**PC 2 (land use)**	**PC 3 (management)**
Depth	**-0.909834**	0.114756	-0.004413
POM $\delta^{15}N$	-0.151646	0.047273	**0.940396**
POM [N] (mg/g dry soil)	**0.828650**	-0.067620	-0.326552
POM $\delta^{13}C$	0.007247	**0.923791**	0.027986
POM [C] (mg/g dry soil)	**0.833253**	-0.064116	-0.328283
Bulk soil $\delta^{13}C$	-0.278611	**0.896773**	0.127468
Bulk soil [C] (%)	**0.916629**	0.304858	-0.069433
Bulk soil $\delta^{15}N$	0.107283	0.574371	**0.641633**
Bulk soil [N] (%)	**0.943493**	0.188811	-0.063915
mOM $\delta^{15}N$	0.132226	**0.700676**	0.584560
mOM [N] (mg/g dry soil)	**0.933666**	0.209823	-0.049806
mOM $\delta^{13}C$	-0.263436	**0.897183**	0.132093
mOM [C] (mg/g dry soil)	**0.897338**	0.350654	-0.027946
POM C:N ratio	**-0.791120**	0.193491	-0.058365
mOM C:N ratio	0.172641	**0.795952**	-0.105743
Bulk soil C:N ratio	0.288676	**0.759473**	-0.157078
η	**-0.725259**	0.368492	-0.132792
mOM/POM $\delta^{13}C$	0.362719	**0.604648**	-0.117529
mOM/POM $\delta^{15}N$	0.123048	0.253007	**-0.770772**
mOM/POM C:N ratio	**0.802927**	0.226895	0.027806
Explained variance (%)	**39.4**	**27.3**	**12.8**

Figure 1
Click here to download high resolution image

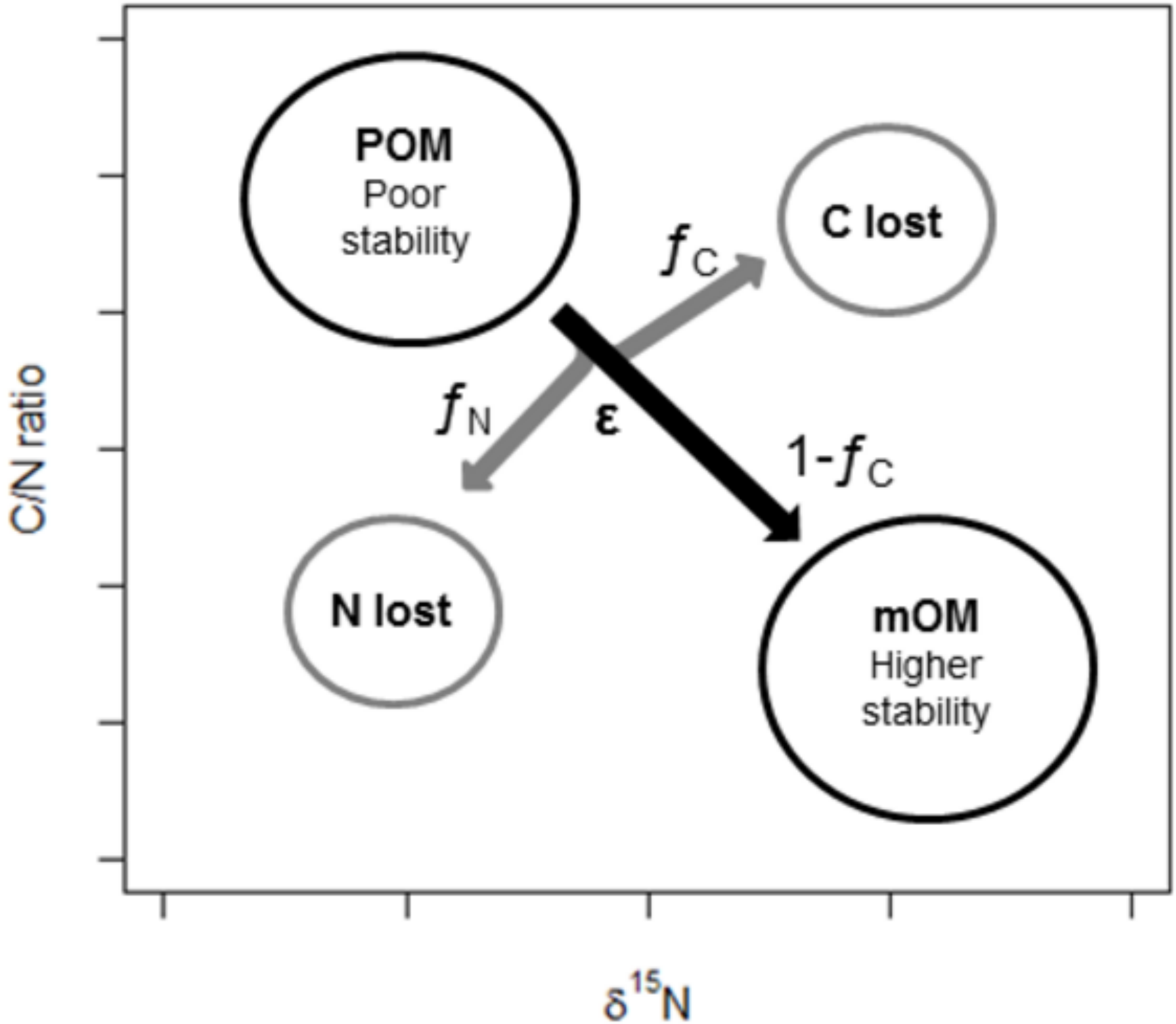

Figure 2

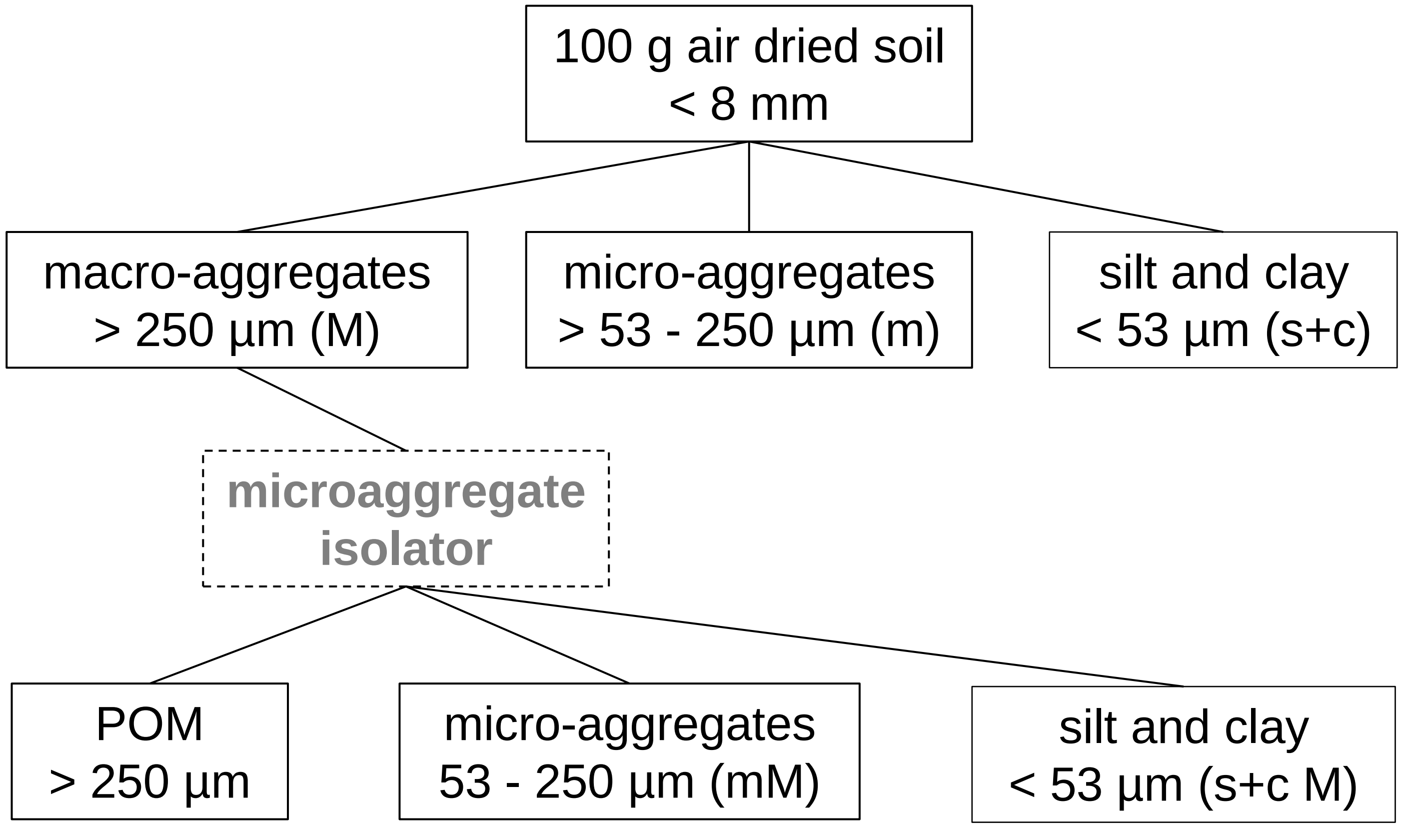
100 g air dried soil
< 8 mm
macro-aggregates
> 250 µm (M)
micro-aggregates
> 53 - 250 µm (m)
silt and clay
< 53 µm (s+c)
microaggregate
isolator
POM
> 250 µm
micro-aggregates
53 - 250 µm (mM)
silt and clay
< 53 µm (s+c M)

Figure 3 (color)
Click here to download high resolution image

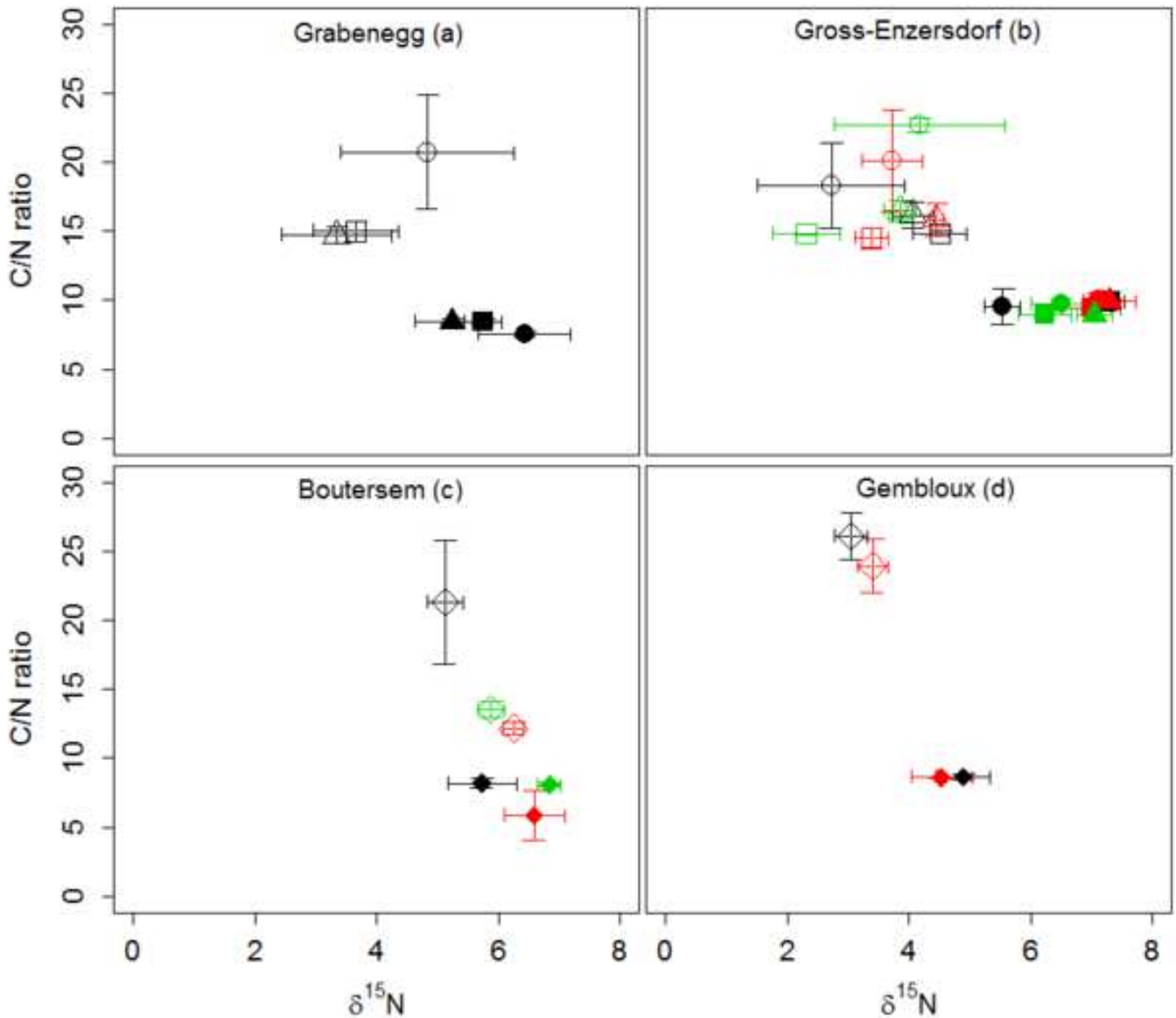

Figure 3 (gray)

Click here to download high resolution image

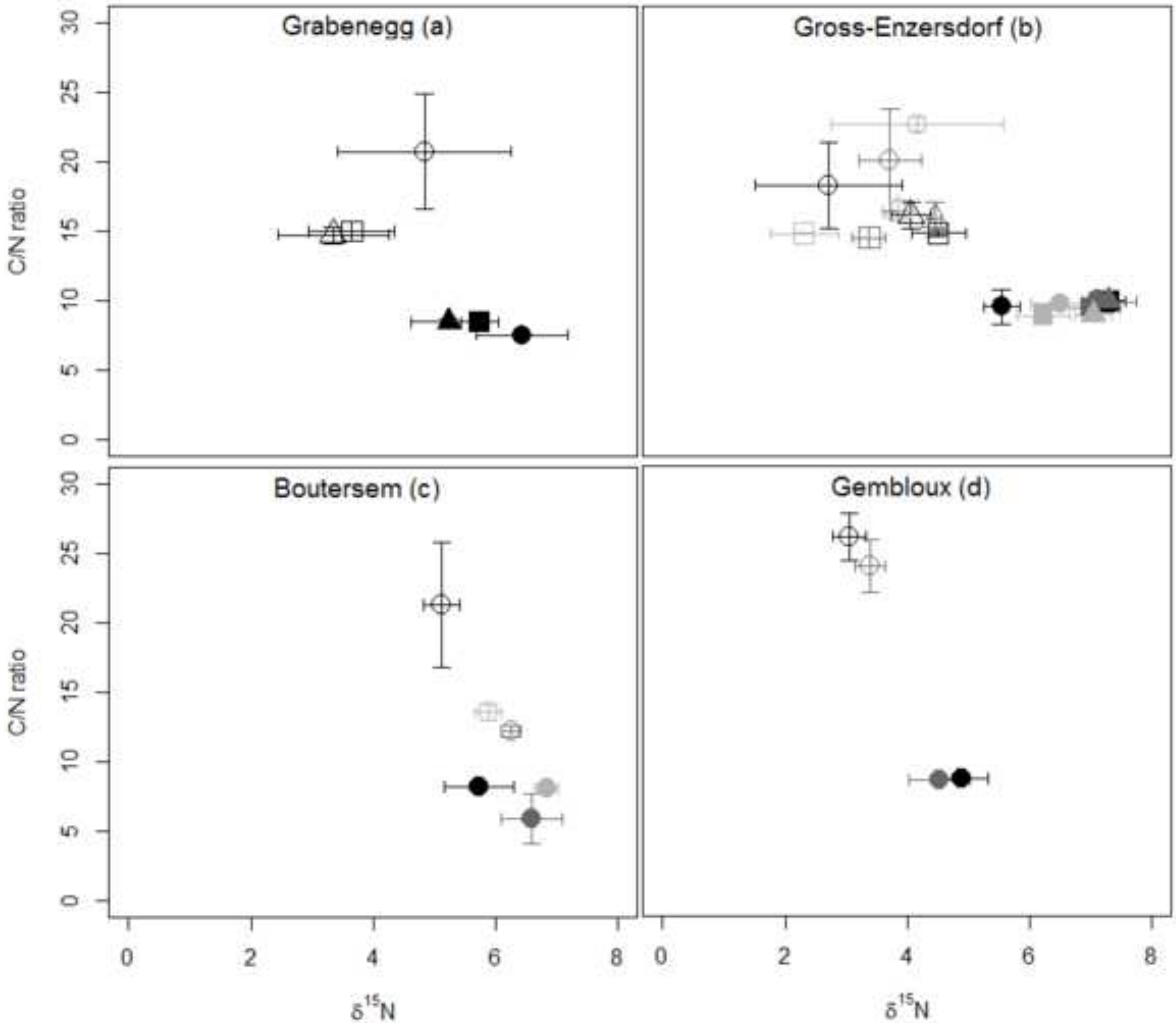

Figure 4 (color)

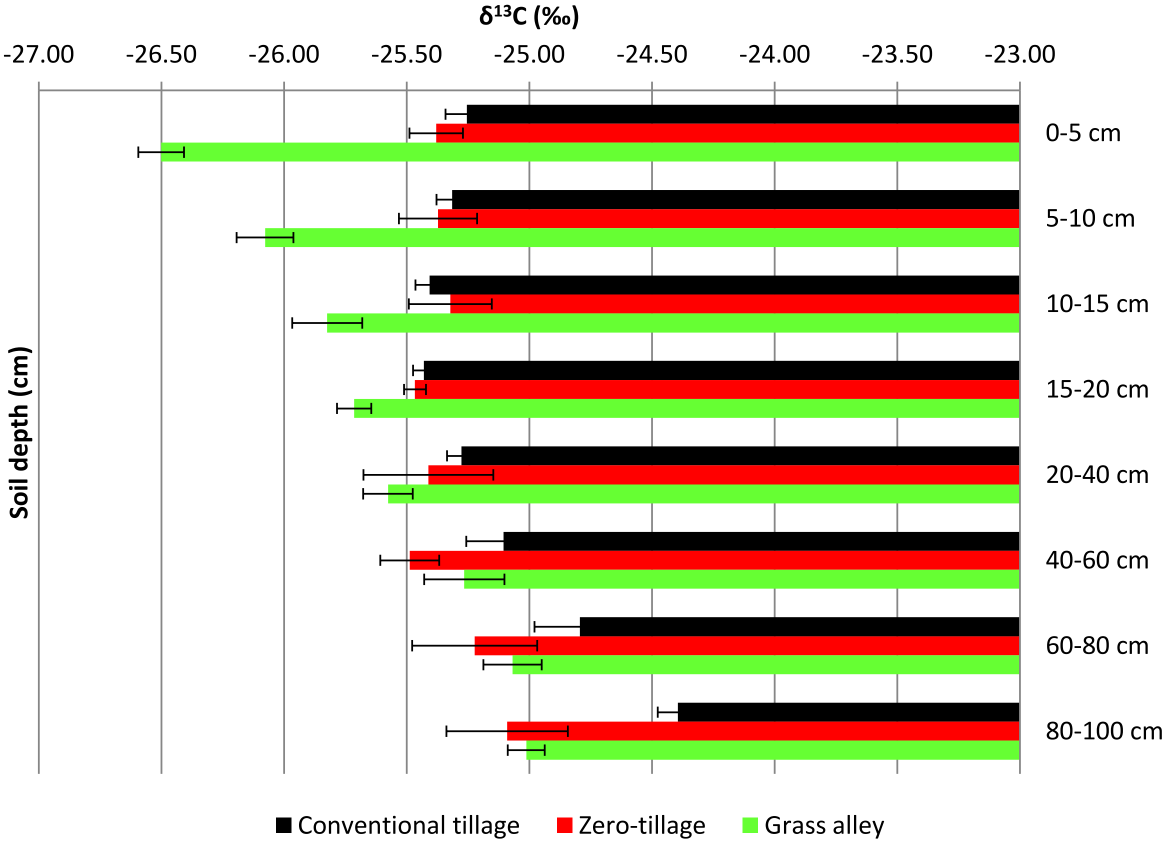

Figure 4 (gray)

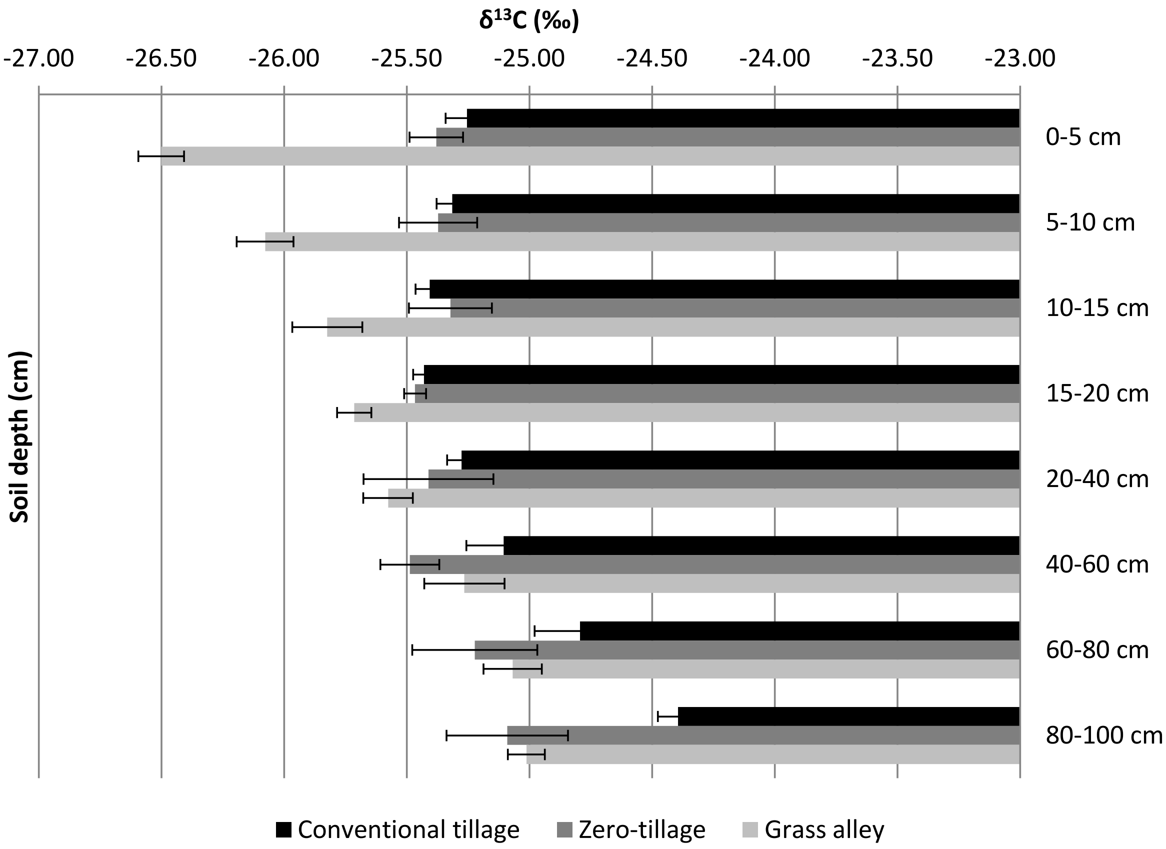

Figure 5 (color)

Click here to download high resolution image

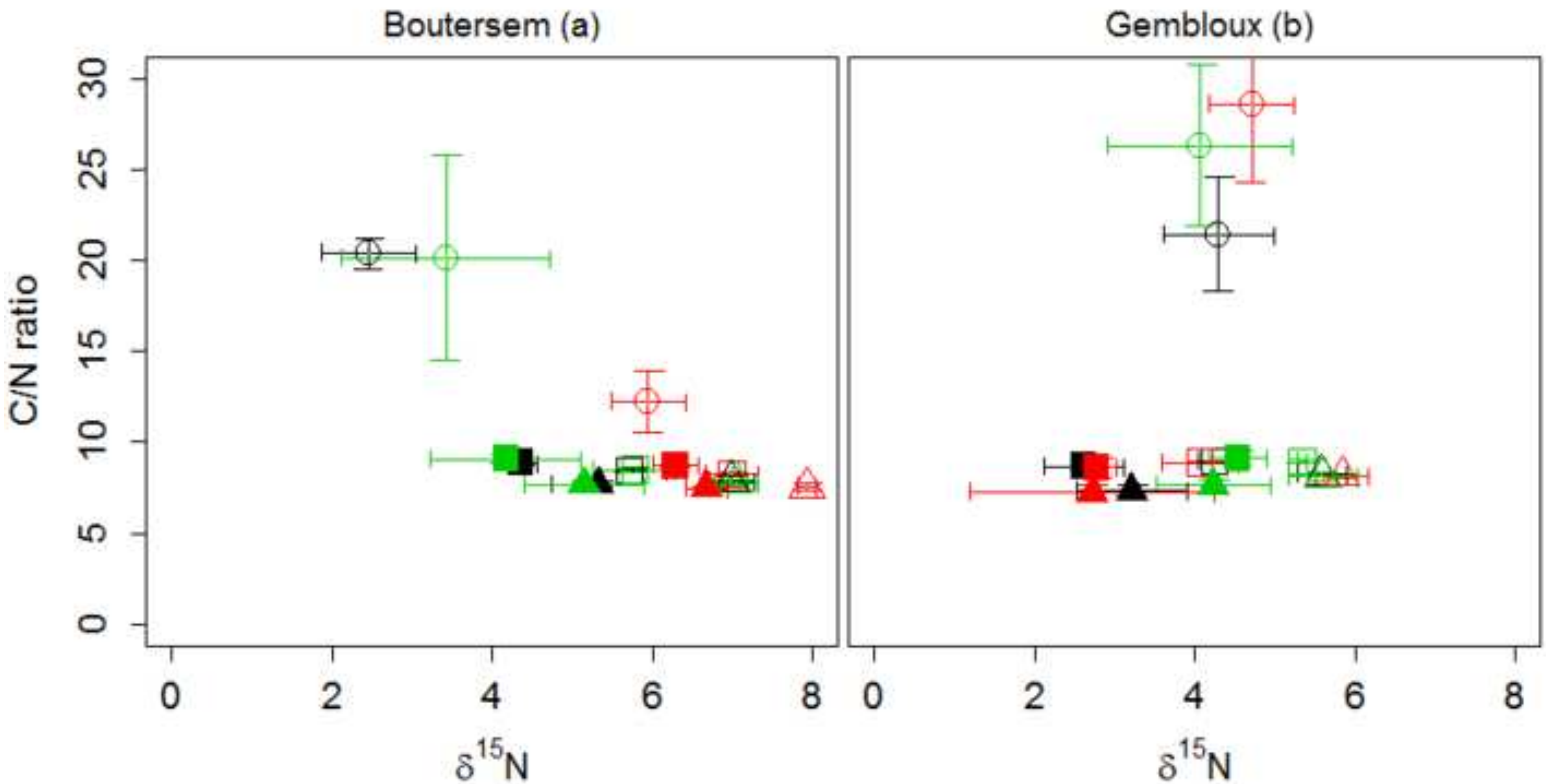

Figure 5 (gray)
Click here to download high resolution image

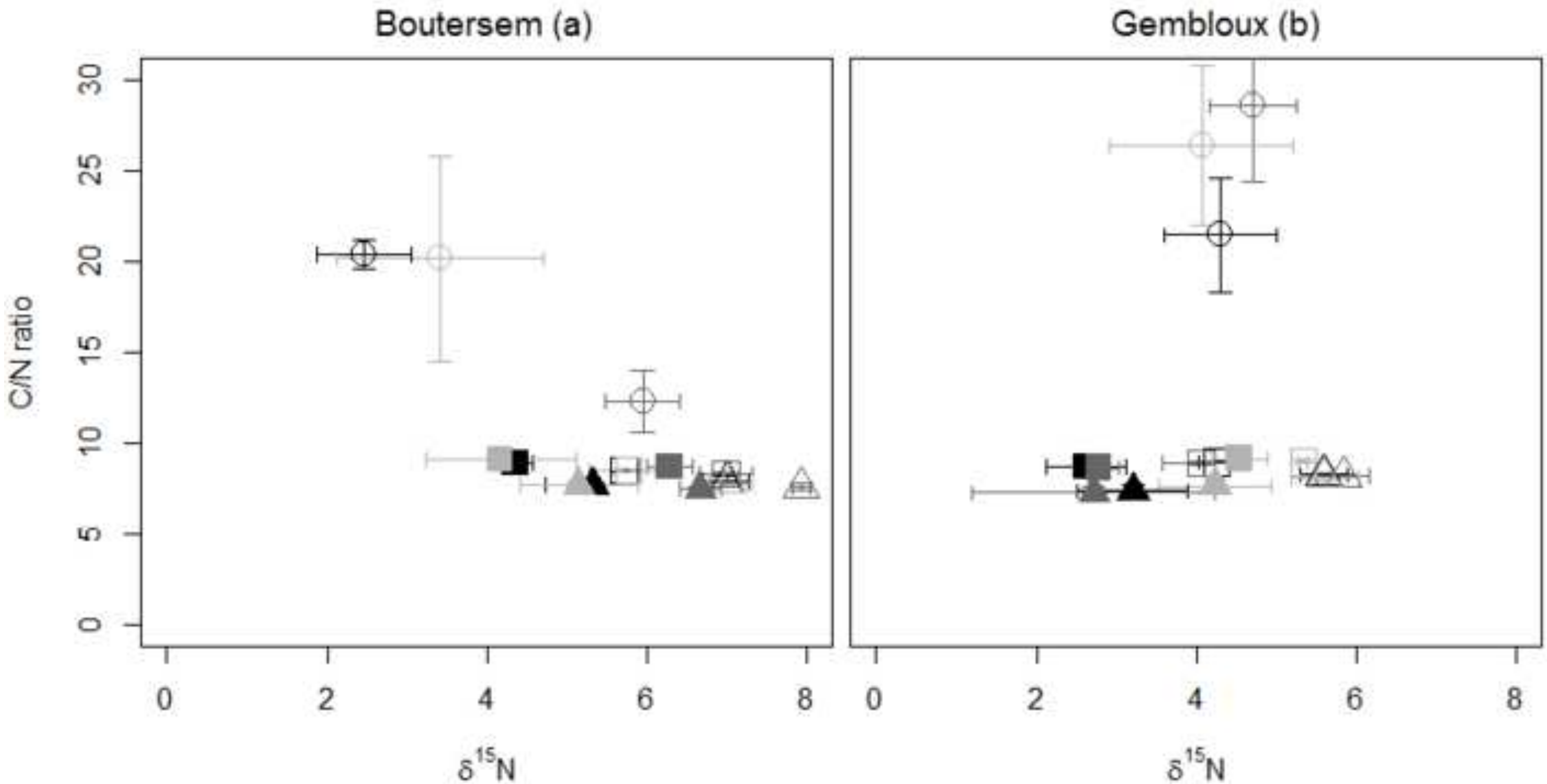

Figure 6 (color)
Click here to download high resolution image

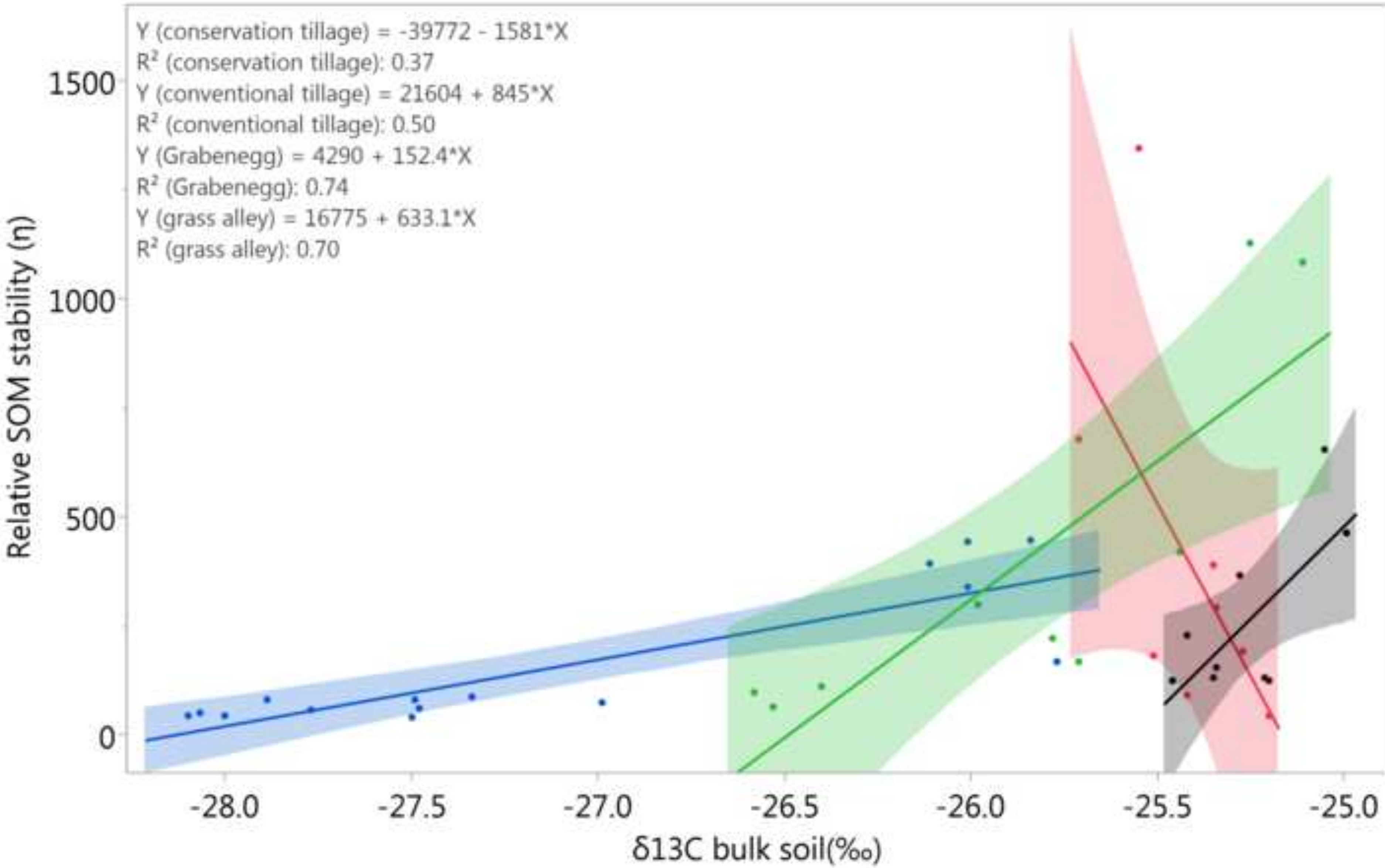

Figure 6 (gray)
Click here to download high resolution image

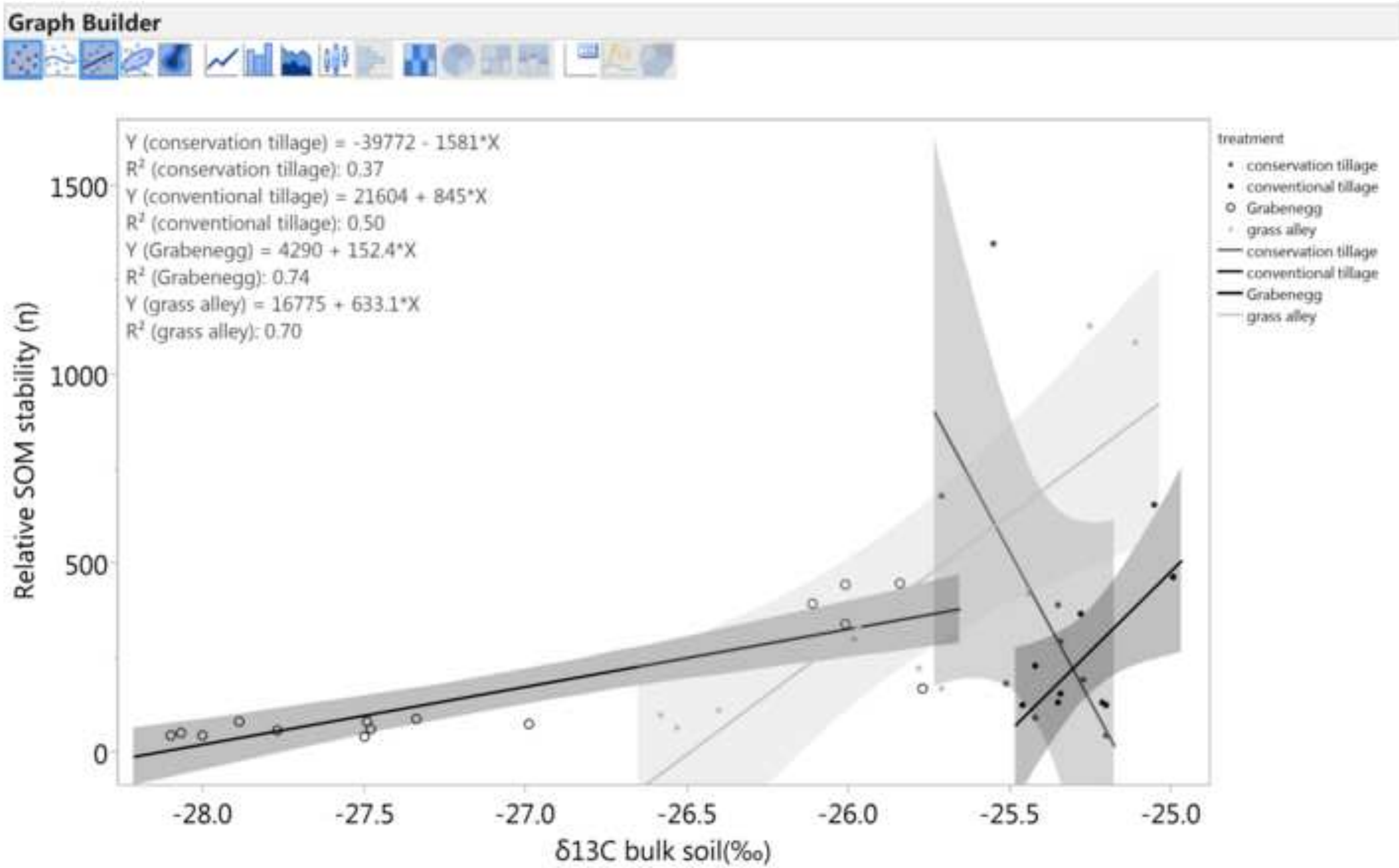

Figure 7 (color)

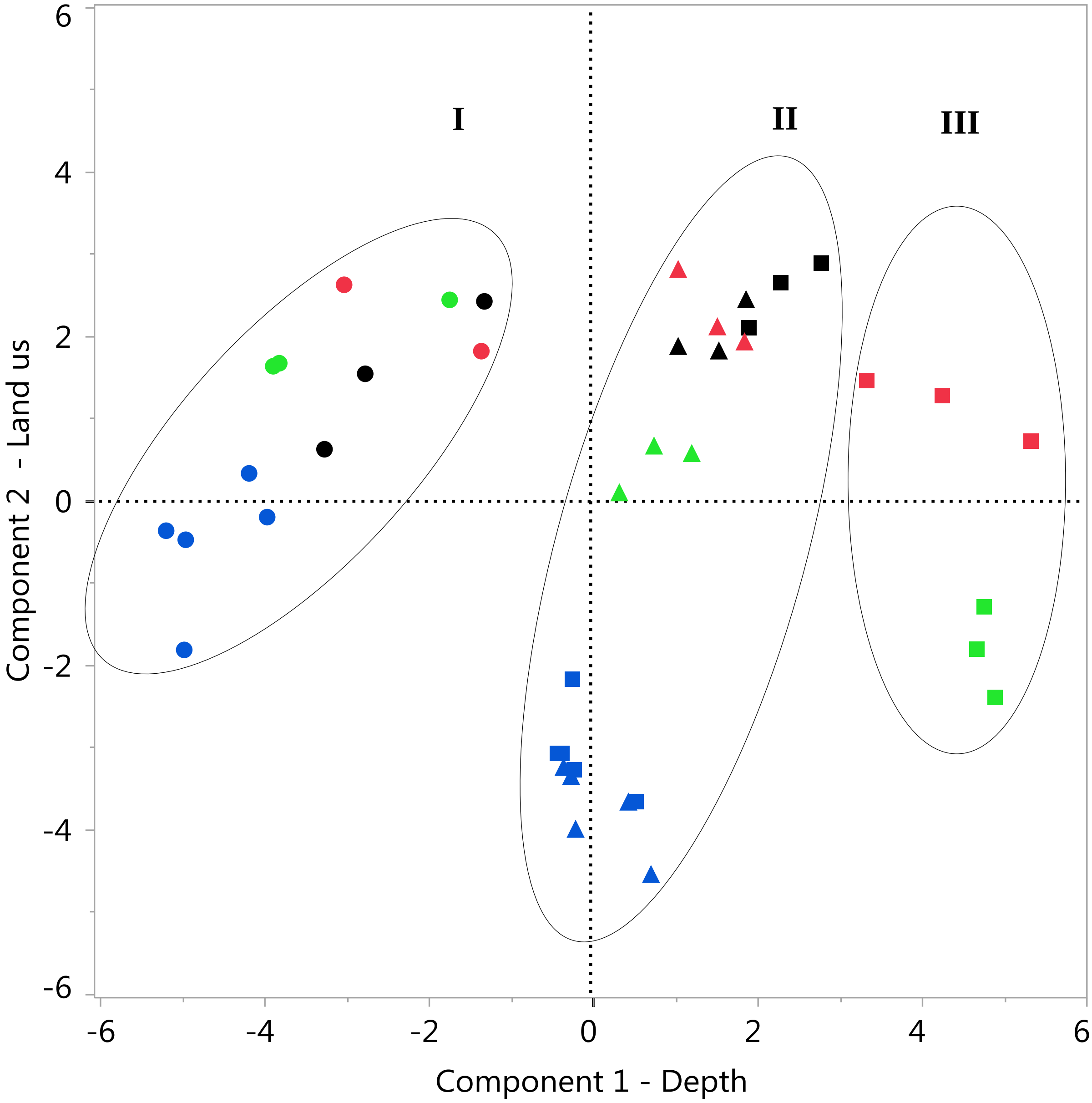

Figure 7 (gray)

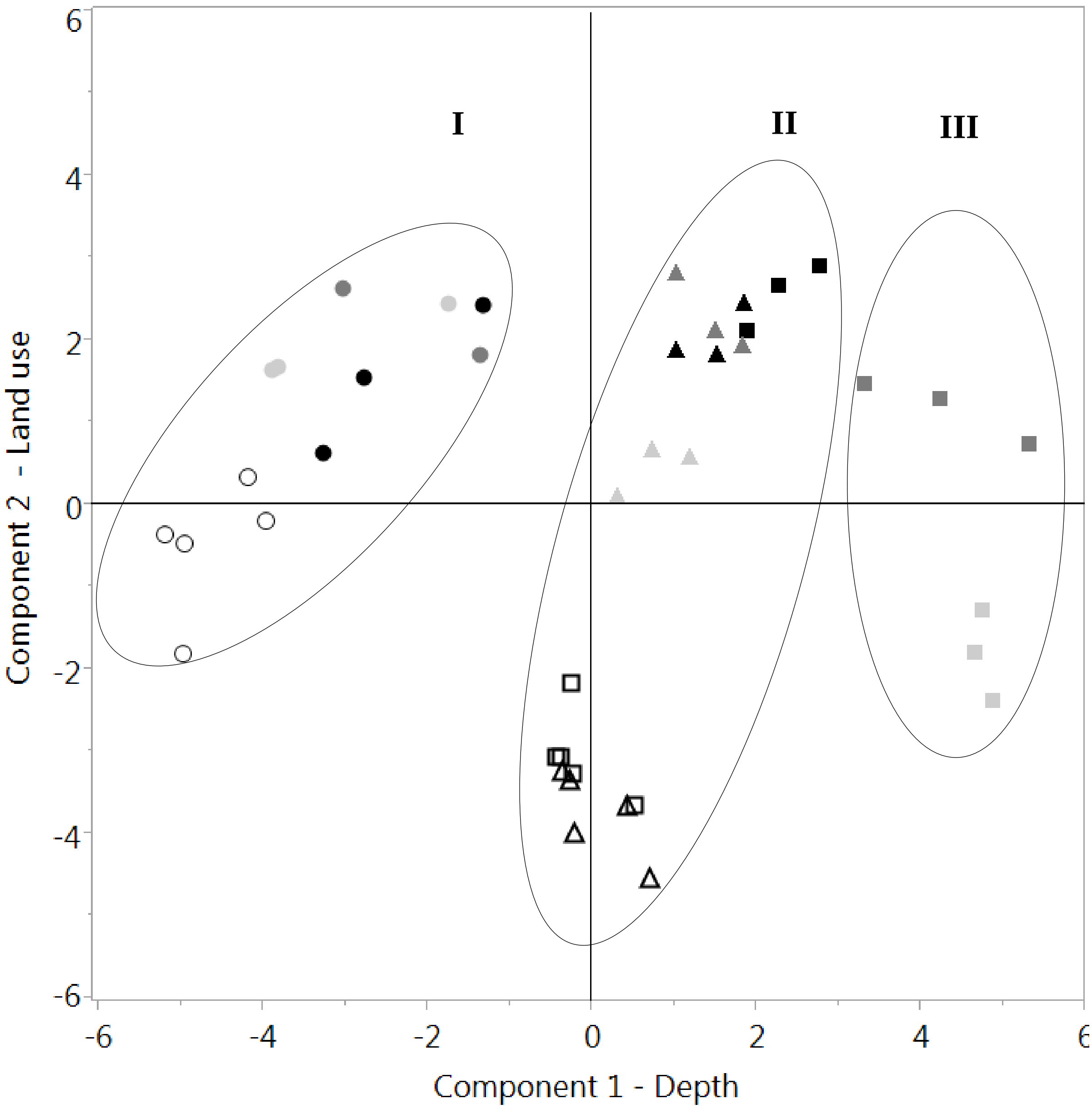

Figure 8 (color)

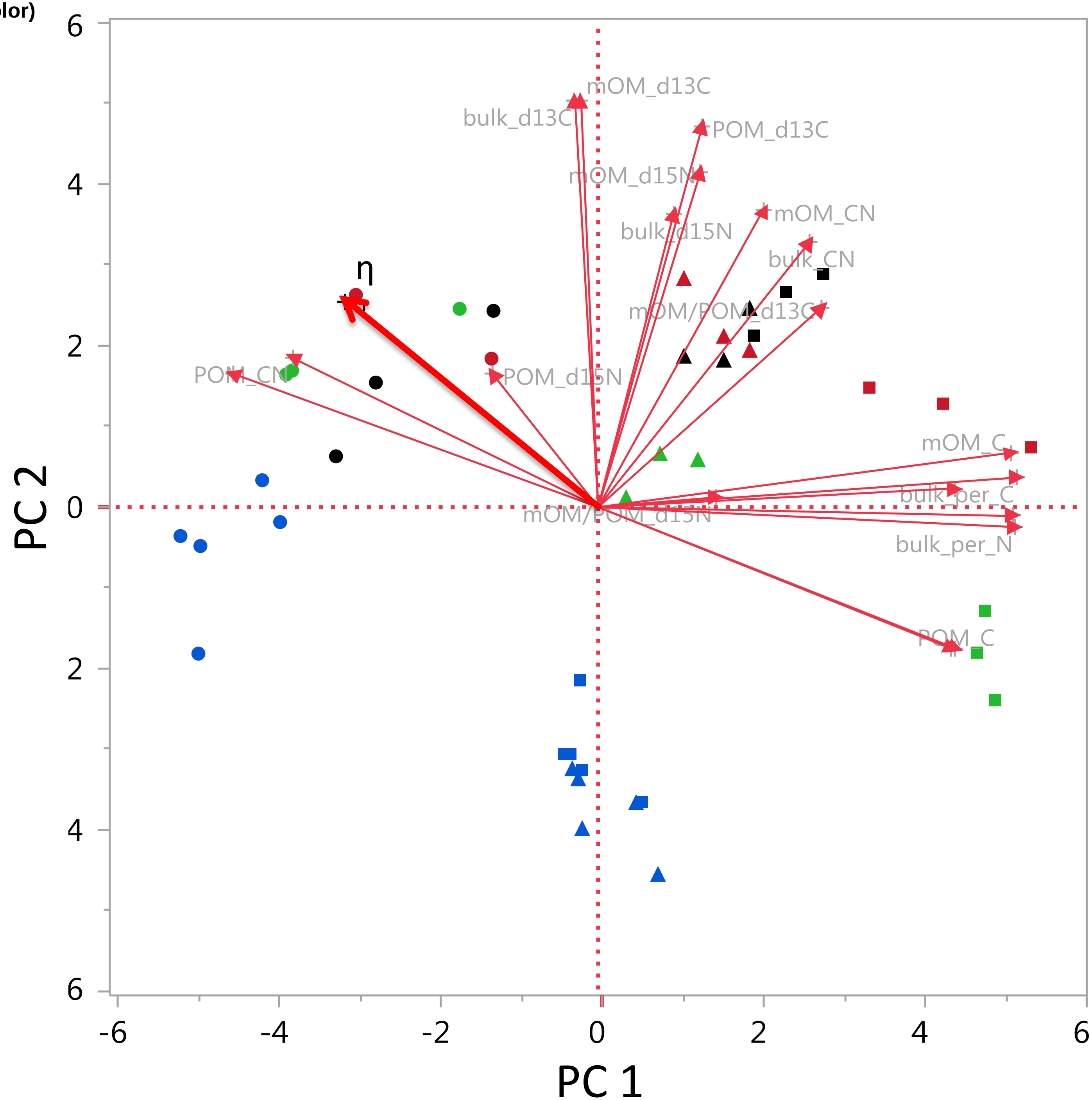

Figure 8 (gray)

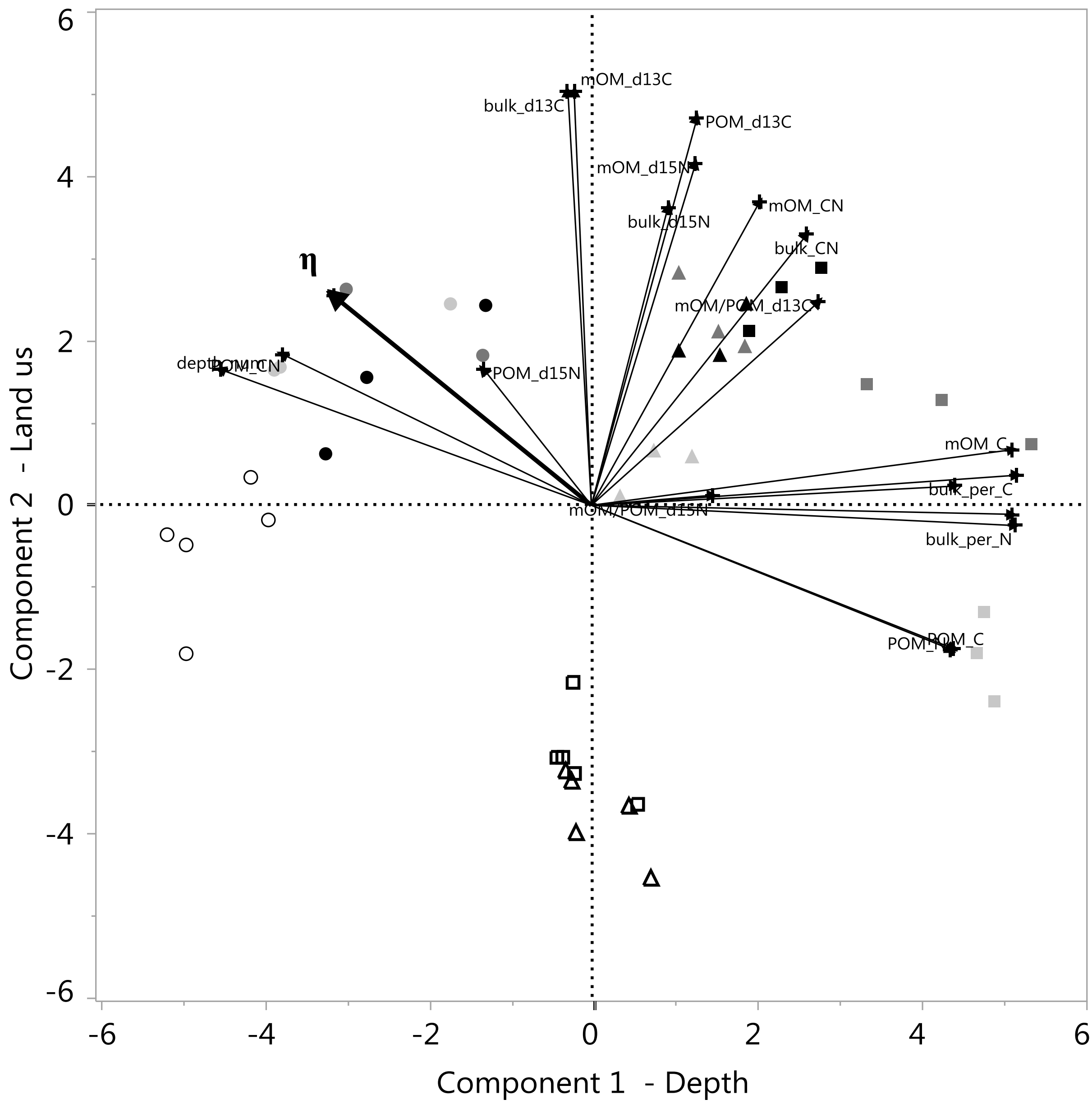

Figure captions

Figure 1: Theoretical evolution of C/N ratio and $\delta^{15}N$ signature for the particulate organic matter (POM) and mineral-associated organic matter (mOM) fraction as described by the model. $f_{N:}$ fraction of N lost, $f_{C:}$ fraction of C lost, ε: fractionation coefficient (Conen et al., 2008).

Figure 2: Fractionation scheme based on Six et al. (2002) dividing the SOM in an unprotected particulate organic matter fraction (POM), two physically protected fractions (m and mM) and two physically and (bio)chemically protected fractions (s+c and s+c M).

Color: **Figure 3:** C/N ratio and $\delta^{15}N$ signature for SOC fractions from the experimental sites in Grabenegg (a), Gross-Enzersdorf (b), Boutersem (c) and Gembloux (d). The POM fraction (open symbols) and mOM fraction (filled symbols) are displayed for four depths (a, b): 0-5cm (□), 10-15cm (Δ), 40-60cm (○) and (c, d): 0-30cm (◊). The error bars indicate the standard deviation. The colors represent various treatments: (b) conventional tillage (black), conservation tillage (red) and grass alleys (green). (c) Control (black), 15t $ha^{-1}y^{-1}$ VFG compost (green) and 45t $ha^{-1}y^{-1}$ VFG compost (red). (d) Control treatment (black) and mulch treatment (red).

Gray: **Figure 3:** C/N ratio and $\delta^{15}N$ signature for SOC fractions from the experimental sites in Grabenegg (a), Gross-Enzersdorf (b), Boutersem (c) and Gembloux (d). The POM fraction (open symbols) and mOM fraction (filled symbols) are displayed for four depths (a, b): 0-5cm (□), 10-15cm (Δ), 40-60cm (○) and (c, d): 0-30cm (◊). The error bars indicate the standard deviation. The colors represent various treatments: (b) conventional tillage (black), conservation tillage (dark-gray) and grass alleys (light-gray). (c) Control (black), 15t $ha^{-1}y^{-1}$

VFG compost (light-gray) and 45t $ha^{-1}y^{-1}$ VFG compost (dark-gray). (d) Control treatment (black) and mulch treatment (dark-gray).

Figure 4: The evolution of the SOC $\delta^{13}C$ signature over a depth profile of 1m for three treatments in the Gross-Enzersdorf experimental site. The error bars indicate the standard deviation.

Color: **Figure 5:** C/N ratio and $\delta^{15}N$ signature for 5 SOC fractions, isolated according to Six *et al*. (2002), from the experimental site in Boutersem (a) an Gembloux (b). The POM fraction (○), free micro-aggregates (□), occluded micro-aggregates (■), free silt & clay (Δ) and occluded silt & clay (▲) fractions are displayed for a depth of 0-30cm. a) Boutersem: the colors represent three treatments: unfertilized control (black), mineral fertilized control (green) and 45t $ha^{-1}y^{-1}$ VFG compost (red). b) Gembloux: the colors represent three treatments: control (black), mulch (red) and mulch with green manure (green). The error bars indicate the standard deviation.

Gray: **Figure 5:** C/N ratio and $\delta^{15}N$ signature for 5 SOC fractions, isolated according to Six *et al*. (2002), from the experimental site in Boutersem (a) an Gembloux (b). The POM fraction (○), free micro-aggregates (□), occluded micro-aggregates (■), free silt & clay (Δ) and occluded silt & clay (▲) fractions are displayed for a depth of 0-30cm. a) Boutersem: the colors represent three treatments: unfertilized control (black), mineral fertilized control (light-gray) and 45t $ha^{-1}y^{-1}$ VFG compost (dark-gray). b) Gembloux: the colors represent three treatments: control (black), mulch (dark-gray) and mulch with green manure (light-gray). The error bars indicate the standard deviation.

Color: **Figure 6:** Bulk soil $\delta^{13}C$ signature to relative stability for the Austrian samples. Regression lines with confidence intervals, equations and R^2 values are displayed for each treatment. The colors represent various treatments: conventional tillage (Gross-Enzersdorf, black), conservation tillage (Gross-Enzersdorf, red), grass alleys (Gross-Enzersdorf, green), ploughed grassland Grabenegg (blue).

Gray: **Figure 6:** Bulk soil $\delta^{13}C$ signature to relative stability for the Austrian samples. Regression lines with confidence intervals, equations and R^2 values are displayed for each treatment. The colors represent various treatments: conventional tillage (Gross-Enzersdorf, black), conservation tillage (Gross-Enzersdorf, dark-gray), grass alleys (Gross-Enzersdorf, light-gray), ploughed grassland Grabenegg (empty symbols).

Color: **Figure 7:** Score plot for component 1 (depth) and component 2 (land use). The scores of the Gross-Enzersdorf and Grabenegg samples are displayed for three depths: 0-5cm (□), 10-15cm (Δ) and 40-60cm (○). The colors represent various treatments: conventional tillage (Gross-Enzersdorf, black), conservation tillage (Gross-Enzersdorf, red), grass alleys (Gross-Enzersdorf, green), ploughed grassland Grabenegg (blue).

Gray: **Figure 7:** Score plot for component 1 (depth) and component 2 (land use). The scores of the Gross-Enzersdorf and Grabenegg samples are displayed for three depths: 0-5cm (□), 10-15cm (Δ) and 40-60cm (○). The colors represent various treatments: conventional tillage (Gross-Enzersdorf, black), conservation tillage (Gross-Enzersdorf, dark-gray), grass alleys (Gross-Enzersdorf, light-gray), ploughed grassland Grabenegg (empty symbols).

Color: Figure 8: Biplot for component 1 (depth) and component 2 (land use). The scores of the Gross-Enzersdorf and Grabenegg samples are displayed for three depths: 0-5cm (□), 10-15cm (Δ) and 40-60cm (○). The colors represent various treatments: conventional tillage (Gross-Enzersdorf, black), conservation tillage (Gross-Enzersdorf, red), grass alleys (Gross-Enzersdorf, green), ploughed grassland Grabenegg (blue). The factor loadings are represented by the red vectors.

Gray: Figure 8: Biplot for component 1 (depth) and component 2 (land use). The scores of the Gross-Enzersdorf and Grabenegg samples are displayed for three depths: 0-5cm (□), 10-15cm (Δ) and 40-60cm (○). The colors represent various treatments: conventional tillage (Gross-Enzersdorf, black), conservation tillage (Gross-Enzersdorf, dark-gray), grass alleys (Gross-Enzersdorf, light-gray), ploughed grassland Grabenegg (empty symbols). The factor loadings are represented by the red vectors.